East European Journal of Physics. 4. 379-385 (2025)
DOI:10.26565/2312-4334-2025-4-35 ISSN 2312-4334

SYNTHESIS OF CdTe QUANTUM DOTS VIA THE MOLECULAR PRECURSOR METHOD AND INVESTIGATION OF THEIR OPTICAL PROPERTIES

Karimberdi E. Onarkulov, Adkhamjon I. Zokirov*
Fergana State University, Fergana, Uzbekistan
**Corresponding Author e-mail: a.zokirov3001@gmail.com*
Received May 23, 2025; revised August 17, 2025; in final form September 15, 2025; accepted September 23, 2025

Cadmium telluride (CdTe) quantum dots (QDs) were synthesizedwere synthesized via a molecular precursor (hot-injection) method and their optical properties were investigated. A cadmium oleate precursor in octadecene/oleic acid was heated to 180 °C under an inert atmosphere, and a trioctylphosphine–tellurium (TOP-Te) solution was swiftly injected to initiate nucleation. By varying the growth time, the QD size was tuned, giving emission colors from green to red. The nanocrystals were characterized by UV–visible absorption and photoluminescence (PL) spectroscopy, which revealed a clear red shift in the optical spectra with increasing particle size. The QDs exhibited size-dependent optical properties consistent with quantum confinement, with the first excitonic absorption peak shifting from approximately 520 nm to 700 nm as the diameter increased. All samples showed high luminescence, with photoluminescence quantum yield (PLQY) values ranging from 60% to 90%. This colloidal synthesis at relatively low temperatures produced colloidally stable QDs with tunable band gaps. These results demonstrate a straightforward route to tailor QD optical properties by controlling the reaction time and provide insights into the growth kinetics and defect states in CdTe QDs.and provide insights into the growth kinetics and defect states in CdTe QDs.
Keywords: *Quantum dot; Cadmium telluride; Molecular precursor; Hot injection; Quantum confinement; Photoluminescence; Absorption; Nanocrystal; Colloidal synthesis; Semiconductor*
PACS: 78.67.Hc, 78.55.Et, 78.30.Fs, 81.07.Ta, 81.16.Be

INTRODUCTION

Quantum dots (QDs) are semiconductor nanocrystals with unique optoelectronic properties that strongly depend on their size [1]. By tuning the particle size, one can tune the absorption and photoluminescence (PL) spectra of QDs – a manifestation of quantum confinement effects [2,3,4]. This size-dependent band gap enables a spectrum of applications in solid-state lighting, display technology, solar cells, and biomedicine [5,6]. Indeed, QDs have been utilized as fluorescent probes in bioimaging, as color converters in LED displays, and as sensitizers in photovoltaic devices, among others [2,3]. The significance of QDs in science and technology was underscored by the awarding of the 2023 Nobel Prize in Chemistry to Ekimov, Brus, and Bawendi for the discovery and synthesis of quantum dots [1]. This achievement highlighted decades of development in colloidal QD synthesis that have led to readily available nanomaterials with high-quality optical properties [9,10].

Colloidal CdTe QDs, in particular, are of great interest as they can emit across the visible spectrum into the near-infrared and have favorable band-gap energies for optoelectronic applications [12,13]. Two of the most common approaches to synthesize CdTe and other II–VI QDs are (1) organometallic (hot-injection) methods in high-boiling organic solvents and (2) aqueous methods with thiol stabilizers [14,15,16]. In a typical organometallic route, a cadmium precursor (e.g., cadmium oleate) in a nonpolar solvent is rapidly injected with a molecular chalcogen source at high temperature, causing burst nucleation followed by nanocrystal growth. This method, introduced in the early 1990s by Murray, Norris and Bawendi, produces nearly monodisperse QDs with excellent crystallinity and optical quality [17]. In contrast, aqueous colloidal synthesis uses water-soluble precursors (e.g., Cd^{2+} salts with NaHTe or TeO_3^{2-} reduced by $NaBH_4$) along with stabilizing thiol ligands such as 3-mercaptopropionic acid (MPA) to obtain QDs at relatively low temperatures (typically 80–100°C) [18]. Both approaches can yield highly luminescent CdTe QDs; however, organometallic methods often produce better size uniformity and higher quantum yields, whereas aqueous methods yield water-dispersible QDs that are more suited for biological applications [19].

The term “molecular precursor method” generally refers to the organometallic hot-injection technique, where a molecular tellurium source (e.g., trioctylphosphine telluride, TOP-Te) is injected into a hot cadmium-containing solution [9]. In this work, we employ the molecular precursor (hot-injection) method to synthesize CdTe QDs at 180 °C, a relatively moderate temperature compared with classical CdSe/CdS syntheses (>300 °C). Our approach emphasizes simplicity and rapid synthesis, allowing us to obtain highly luminescent CdTe QDs within minutes. The emission color can be tuned from green to red by adjusting the reaction time. While similar hot-injection strategies for CdTe have been reported (including the use of single-molecule precursors, such as cadmium diphenylditelluride, in coordinating solvents) [9,20], this study focuses on a straightforward TOP-Te injection into a cadmium oleate solution. We also compare our results with alternative recent techniques; for instance, microwave-assisted aqueous syntheses have achieved tunable emission of thioglycolic acid (TGA)-capped CdTe QDs by varying reaction time and conditions [21]. In this paper, we detail the synthesis of CdTe

Cite as: K.E. Onarkulov, A.I. Zokirov, East Eur. J. Phys. 4, 379 (2025), https://doi.org/10.26565/2312-4334-2025-4-35

QDs via the molecular precursor method, characterize their size-dependent optical properties, and discuss the quantum confinement effects observed.

METHODS

Cadmium oxide (CdO, 99.99%), oleic acid (OA, technical grade, 90%), 1-octadecene (ODE, 90%), and trioctylphosphine (TOP, 90%) were used as received. Tellurium powder (99.999%) was used. All synthesis manipulations were carried out under an inert atmosphere (argon) using standard air-free techniques to prevent oxide formation.

Preparation of precursors: Cadmium oleate, the Cd precursor, was prepared in situ by heating CdO with excess oleic acid in ODE. In a three-neck round-bottom flask, CdO (13 mg, ~0.10 mmol), OA (~0.6 mL, 1.9 mmol), and ODE (10 mL) were combined. The mixture was heated to 120°C under vacuum for 30 min to remove moisture and dissolved gases, then purged with argon. The temperature was then raised to 180 °C, at which point the CdO had completely reacted with OA to form cadmium oleate (yielding a clear solution). Separately, a TOP-Te precursor solution was prepared by reacting Te powder with TOP. Approximately 13 mg of Te (0.10 mmol) was added to 1 mL of TOP in a small flask and heated (under Ar) to ~200 °C until the Te dissolved, yielding a clear amber-colored TOP-Te solution.

Synthesis of CdTe QDs: Once the cadmium oleate solution reached 180 °C, the TOP-Te solution (1 mL) was swiftly injected into the hot Cd-oleate/ODE solution, marking time zero for QD nucleation. The reaction mixture was vigorously stirred and maintained at 180 °C for the duration of nanocrystal growth. Aliquots were withdrawn at specific reaction times (3, 7, 9, and 16 min) to obtain CdTe QD samples. Growth was quenched by rapidly cooling each aliquot to room temperature (e.g., by an ice-water bath). No additional shell was added; the native oleate ligand matrix was relied upon to passivate and stabilize the QD surfaces. The following simplified reaction equations summarize the precursor formation and QD nucleation steps:

$$CdO + 2OA \xrightarrow{180°C} Cd(OA)_2 + H_2O, \quad (1)$$

$$Te(s) + TOP \xrightarrow{200°C} TOP - Te\ (solution), \quad (2)$$

In the above, OA represents oleic acid and TOP-Te denotes trioctylphosphine telluride (a molecular Te complex in solution). Upon injection of TOP-Te into the hot Cd(OA)_2/ODE solution (Equation 2), CdTe nuclei form and then grow as the reaction progresses. During growth, the solution's color visibly changes: initially nearly colorless immediately after nucleation, then pale yellow, orange, and finally dark red as the nanocrystals enlarge – indicating a progressive shift of the absorption edge to longer wavelengths.

After the desired reaction time, the QDs were isolated by a standard purification procedure. Specifically, an aliquot was removed from the hot reaction mixture and mixed with anhydrous ethanol (to induce precipitation of the QDs and remove excess ligands/byproducts), then centrifuged to collect the QD precipitate. The precipitated QDs were redispersed in a nonpolar solvent (hexane or toluene). This precipitation/redispersion wash was repeated twice to yield clean, stable colloidal CdTe QDs capped with oleic acid. All samples were stored in sealed vials under inert gas (argon) in the dark. The molar concentration of each QD dispersion was estimated via the Beer–Lambert law at the first excitonic absorption maximum, $c = A/(\varepsilon l)$, with $l = 1.00\ cm$. The size-dependent molar extinction coefficient ε for CdTe QDs was taken from literature; we used the empirical CdTe relation $\varepsilon = 10043D^{2.12}$ ($M^{-1}\ cm^{-1}$), where D is the TEM/optically estimated diameter in nm.

Characterization: UV–Vis absorption spectra were collected on a double-beam spectrophotometer with hexane as both solvent and reference. Photoluminescence (PL) spectra were recorded on a fluorescence spectrometer ($\lambda_{exc} = 350\ nm$; 1 cm quartz cuvettes; room temperature) and are reported without detector-response correction, as our analysis focuses on peak positions and qualitative line shapes. The absorbance and PL intensity scales were verified with a calibrated tungsten lamp and a silicon photodiode, respectively.

PL quantum yields (PLQY) were determined by the relative method using quinine sulfate in 0.1 M H_2SO_4 (literature $\Phi \approx 54\%$) as the standard. The standard and QD dispersions were prepared to have matched absorbance at 350 nm ($A \approx 0.05–0.10$) and were measured under identical integration settings. For each sample, PLQY was obtained from the slope of integrated emission vs. absorbance, averaged over three independently prepared dispersions. All optical measurements (absorbance, PL, PLQY) were acquired in triplicate and are reported as mean ± standard deviation.

Colloidal dispersions were also inspected visually under ambient light and 365 nm UV to assess emission color and any qualitative signs of precipitation. Transmission electron microscopy (TEM) and X-ray diffraction (XRD) were used to determine particle size, morphology, and crystal structure. For TEM, a drop of the hexane dispersion was cast onto a carbon-coated copper grid, dried under ambient conditions, and imaged at 200 kV. For XRD, purified QDs were drop-cast onto glass to form a thin film and measured on a powder diffractometer with Cu Kα radiation (λ = 1.5406 Å) over 2θ = 20°–60°; peak positions were compared with reference CdTe patterns to confirm phase identity and estimate crystallite size.

RESULTS

Optical appearance and qualitative emission: Figure 1 is a schematic illustration of the CdTe QD synthesis via the molecular precursor method. After injection and during growth (0–16 min), the solution color evolves from nearly

colorless (immediately after nucleation) to yellow, orange, and finally red, corresponding to increasing QD size and a red-shifting band gap. This color change is apparent in the actual QD samples. Figure 2a shows photographs of vials containing CdTe QD dispersions (in hexane) under normal ambient light for four different reaction durations (from left to right: 3 min, 7 min, 9 min, 16 min). The solution color deepens with longer synthesis time: the 3 min sample is nearly colorless with only a faint yellow tint, while the 16 min sample is visibly reddish-brown. This progression indicates the growth of larger CdTe nanoparticles, since larger QDs have narrower band gaps and thus absorb more lower-energy (visible) light, imparting a stronger color to the solution. Figure 2b presents the same set of samples under ultraviolet illumination (365 nm). A striking rainbow of fluorescence is observed: the shortest reaction (smallest QDs) emits green light, and as the QD size increases, the emission color shifts through yellow and orange to red for the largest QDs. All samples show bright, saturated fluorescence, confirming efficient surface passivation by the oleic acid ligands. The emission colors correspond roughly to the expected PL peak wavelengths for CdTe QDs of these sizes (approximately 520–540 nm for the green-emitting smallest dots, 580–600 nm for medium-sized QDs emitting yellow-orange, and ~640–680 nm for the red-emitting largest dots). These qualitative observations already suggest successful tuning of QD size via reaction time, consistent with quantum confinement theory [18].

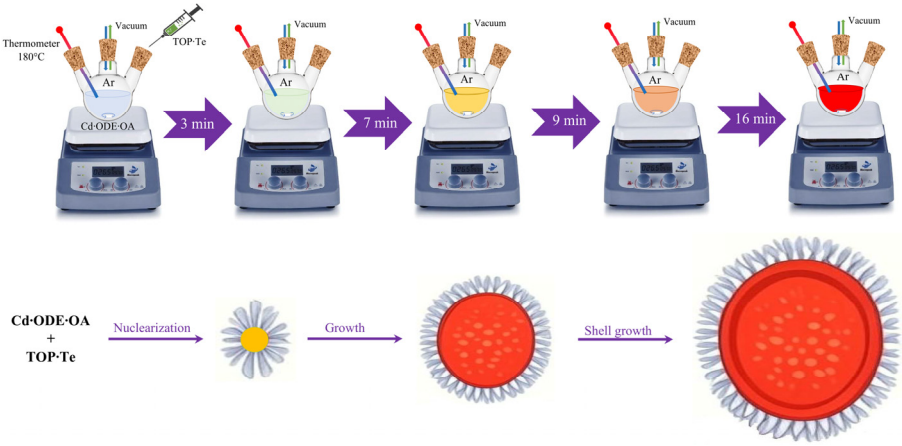

Figure 1. Schematic illustration of the CdTe QD synthesis via the molecular precursor method

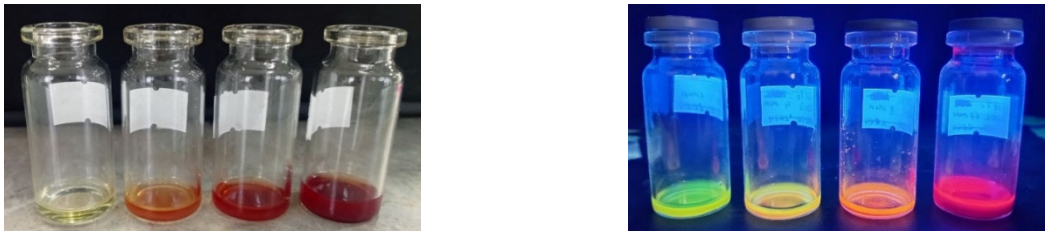

a b

Figure 2. Photographs of CdTe QD samples at various reaction times, showing (a) solution color under ambient light and (b) photoluminescence under 365 nm UV light

UV–Vis absorption spectra: Figure 3 shows the UV–Vis absorption spectra of the CdTe QD samples (dispersed in hexane) for the four different growth times.

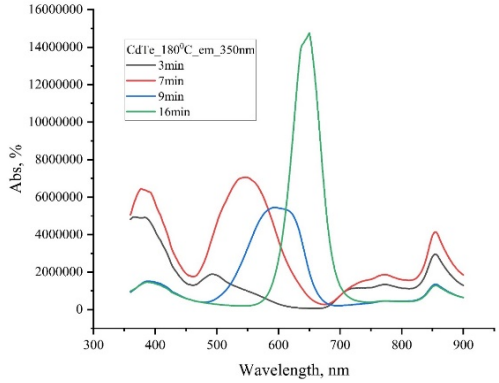

Figure 3. UV–Vis absorption spectra of CdTe QDs (in hexane) grown at 180 °C with different reaction times (black: 3 min; red: 7 min; blue: 9 min; green: 16 min)

All spectra exhibit a distinct first excitonic absorption peak, a hallmark of quantum-confined semiconductor nanocrystals. For the 3 min sample (black curve), the first absorption peak appears around 500–520 nm (in the blue-green

region). With increasing growth time, this peak systematically shifts to longer wavelength: approximately 560 nm for the 7 min sample (red curve), ~620 nm for the 9 min sample (blue curve), and ~700 nm for the 16 min sample (green curve). Concomitantly, the absorption edge (onset of strong absorption) moves from roughly 550 nm (3 min sample) to about 800 nm (16 min sample). This pronounced red-shift of the absorption features clearly indicates an increase in particle size over the reaction interval. Longer reaction times allow the initially formed CdTe nuclei to grow larger, resulting in reduced quantum confinement and thus a smaller effective band gap. The observed absorption peak positions are in good agreement with literature values for CdTe QDs in the ~2–5 nm size range. For instance, the 16 min sample's first exciton peak at ~700 nm is consistent with QDs about 4–5 nm in diameter, whereas the 3 min sample's peak near 500 nm corresponds to very small nanocrystals of around ~2 nm diameter. These size estimates are supported by the qualitative PL colors in Figure 2b and by empirical sizing formulas reported in previous studies [18].

Photoluminescence spectra: Photoluminescence spectra of the same four CdTe QD samples are shown in Figure 4. Under 350 nm UV excitation, the emission maxima exhibit a parallel red-shift with increasing reaction time, mirroring the absorption trend in Figure 3. Specifically, the PL peak moves from ~525 nm for the 3 min QDs to ~580 nm (7 min), ~630 nm (9 min), and ~650–670 nm for the 16 min QDs. Each spectrum consists of a single prominent emission band; we did not observe any secondary long-wavelength emission bands (within the detection limit), indicating an absence of significant trap-state luminescence. The PL full-width at half-maximum (FWHM) for all samples is on the order of 30–50 nm, which is relatively narrow. Such narrow emission peaks suggest a fairly uniform QD size distribution (narrow size polydispersity) and good crystallinity. The Stokes shift (the difference between the absorption peak and PL peak) remains modest (~20–30 nm for these samples), which further indicates effective surface passivation with minimal defect-related Stokes losses. The qualitative brightness observed under UV illumination (Figure 2b) is reflected in the PL spectra intensity; all samples were highly emissive. We note that although we did not perform time-resolved PL measurements, the absence of any low-energy (red/NIR) trap emission in steady-state PL implies that radiative recombination is primarily via band-edge exciton decay. A detailed study of recombination lifetimes (e.g., via time-resolved PL) would be valuable future work to confirm this and to quantify carrier dynamics in these QDs.

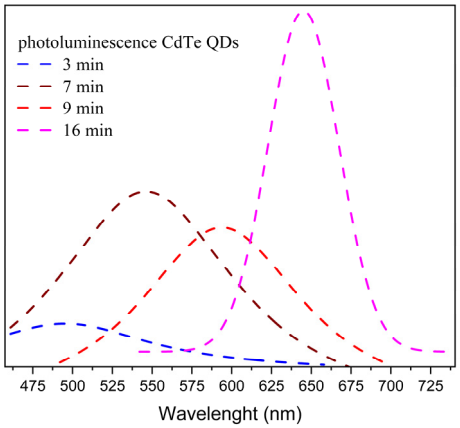

Figure 4. Photoluminescence (PL) spectra of CdTe QDs grown at 180 °C for 3, 7, 9, and 16 min. All samples were measured in hexane at room temperature (excitation: 350 nm).

Photoluminescence quantum yield: In addition to qualitative brightness, we quantitatively evaluated the photoluminescence efficiency of the QDs. PL quantum yield (PLQY) values for all samples, measured relative to a quinine sulfate standard, are summarized in Table 1.

Table 1. Photoluminescence characteristics of CdTe QDs as a function of reaction time.

Growth time	λ_{em} (nm)	Diameter (nm)	Absorbance A	ε ($M^{-1}\cdot cm^{-1}$)	Concentration (μM)	PL FWHM (nm)	Stokes shift (nm)	PLQY (%)
3 min	525	2.0	0.045	43.656	1.03	47	25	88.9 ± 2.5
7 min	580	3.5	0.051	142.984	0.36	50	20	63.9 ± 3.1
9 min	630	4.0	0.061	189.771	0.32	53	30	61.9 ± 4.0
16 min	670	5.0	0.043	304.565	0.14	54	20	64.0 ± 3.7

The 3 min CdTe QDs exhibited the highest PLQY, around ~89%. The intermediate-sized QDs (7 min and 9 min samples) showed slightly lower PLQYs (~64% and ~62%, respectively), and the largest QDs (16 min) had a PLQY of ~64%. All samples thus have moderately high quantum yields (exceeding 60%), even without any core/shell structure. The trend of decreasing PLQY with increasing QD size could be due to a greater likelihood of crystalline imperfections or surface defects in the larger nanocrystals, or reabsorption effects in samples with more red-shifted emission. Conversely, the smallest QDs may have fewer nonradiative surface recombination centers relative to their volume, thanks to the strong binding of oleate ligands. Regardless of the exact mechanism, these QY values indicate that the CdTe cores synthesized by this method are of good optical quality. We anticipate that adding an epitaxial shell (e.g., ZnS) around

these cores would further enhance the PLQY and stability, as has been observed in core-shell QD systems; however, this is beyond the scope of the present work.

We quantified the QD number concentration from the UV–Vis spectra using the Beer–Lambert law at the first excitonic peak and a size-dependent extinction coefficient for CdTe QDs. The diameters used in ε(D) were taken from TEM (and cross-checked against the excitonic peak positions). Table 1 summarizes the results for the 3-, 7-, 9-, and 16-minute samples.

These values (≈0.14–1.03 μM) are typical for colloidal QD dispersions prepared in nonpolar solvents and are sufficiently dilute to minimize inner-filter and reabsorption artifacts during optical measurements.

Growth and reproducibility: Nucleation began almost immediately upon TOP-Te injection, as evidenced by an instantaneous color change to pale yellow. Thereafter, the absorption edge and PL maximum red-shifted progressively with time as the nanocrystals grew. By ~16 min, growth slowed markedly, consistent with precursor depletion and the onset of Ostwald ripening. No secondary nucleation was detected after the initial burst, in line with the classical LaMer mechanism for achieving narrow size distributions. All samples were time-stamped aliquots from a single batch, and their consistent optical trends confirm reproducible, well-controlled growth.

Our results align well with other reports on CdTe QD growth. For example, da Costa et al. (2024) monitored CdTe QD formation in situ. They found that emission peaks shifted from ~550 nm to ~655 nm as reaction time or temperature increased, corresponding to QD diameters growing from ~2 nm (green-emitting) to ~4 nm (red-emitting). This is in excellent agreement with the size progression achieved in our study. Such consistency confirms that the molecular precursor (TOP-Te) method effectively produces CdTe QDs whose size can be tuned predictably by reaction time, similar to the control achieved by adjusting temperature or precursor ratios in other synthesis methods [18].

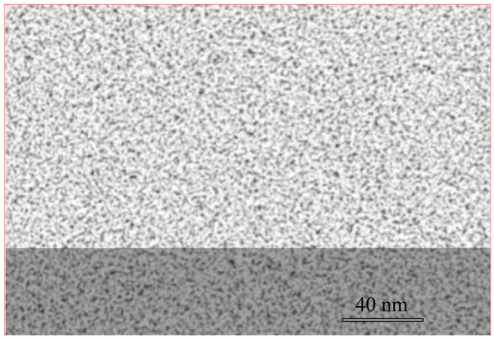

Figure 5. TEM image of the synthesized CdTe QDs (representative sample) showing nearly spherical nanocrystals with an average diameter of ~4 nm (scale bar: 40 nm)

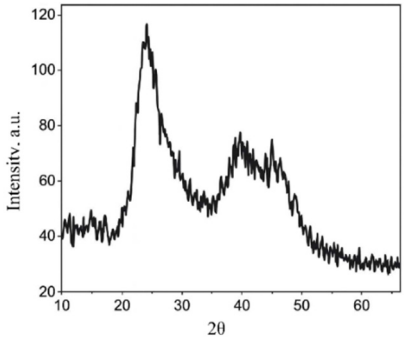

Figure 6. XRD pattern of a purified CdTe QD sample, confirming the crystalline zinc-blende CdTe structure

The above results demonstrate a clear correlation between reaction time, particle size, and optical properties for CdTe QDs synthesized by the molecular precursor (hot-injection) method. Short reaction times yield small QDs that absorb and emit in the blue-green region, whereas longer times produce progressively larger QDs with red-shifted spectra. This behavior is a direct consequence of quantum confinement: smaller nanocrystals confine charge carriers in a tighter volume, raising their kinetic energy and thus increasing the energy of optical transitions [1]. As the CdTe QDs grow, the confinement energy decreases, leading to lower band-gap energies and emission at longer wavelengths (approaching the bulk CdTe band edge of ~820 nm). Our experimental data (Figures 2–4) vividly illustrate this tunability, which is one of the defining advantages of colloidal QDs.

It is worth noting some practical benefits of the synthetic approach we used. The reaction is rapid – within a few minutes, a spectrum of sizes (and colors) can be obtained – and it occurs at 180 °C, which is a relatively low temperature compared to many classic organometallic syntheses of II–VI QDs (often ≥300 °C for CdSe or CdS). A lower synthesis temperature simplifies the experimental setup and can reduce unwanted side reactions or precursor degradation. In our case, the moderate temperature was sufficient because TOP-Te is a highly reactive Te source that readily reacts with cadmium oleate even at 180 °C. This is in contrast to some older methods, where, for example, elemental Te would have to be injected into a 300°C solvent, or where cadmium precursors, such as $CdCl_2$, had to be reduced in situ with $NaBH_4$ in an aqueous solution [18]. By using pre-formed Cd–oleate and a molecular Te precursor (TOP-Te), we bypassed the need for an external reducing agent and leveraged the reactivity of organometallic precursors to achieve CdTe formation under milder conditions.

Another advantage of our approach is the monodispersity observed in the QD samples. The relatively narrow absorption peaks (Figure 3) and the vivid, narrow emission bands (Figure 4 and visually in Figure 2b) indicate a uniform QD size distribution for each sample. This can be attributed to the classic hot-injection mechanism, promotes a burst of nucleation followed by focused growth on existing seeds, rather than continuous nucleation. Our observation that no new nucleation occurred after the initial stage (with aliquots taken at later times yielding larger QDs but no significant second population of small QDs) supports the notion of effective Ostwald ripening and growth on seed crystals only [9]. In practice, this means one can simply stop the reaction at a desired time to obtain QDs of a target emission wavelength – a convenient way to tune QD color by controlling reaction duration.

We also briefly compare our results with the aqueous route for CdTe QD synthesis. While not the focus of this study, it is known that aqueous-synthesized CdTe QDs (typically using thiol ligands like MPA) generally require longer reaction times (on the order of hours) to achieve similar emission wavelengths, and often the size distribution is broader than that of hot-injection QDs [1]. However, a key benefit of aqueous QDs is that they are directly obtained as water-soluble colloids. In contrast, the oleic-acid-capped QDs we produced are hydrophobic (soluble only in nonpolar organic solvents). We did not perform a ligand exchange to water in this work, but we acknowledge its importance. In fact, recent studies have shown that microwave-assisted aqueous synthesis can produce CdTe QDs with controlled emission by varying parameters [21], offering a complementary, more environmentally benign approach. Exploring ligand exchange or direct aqueous synthesis for our QDs is an important future direction to extend their applicability.

The optical quality of our CdTe QDs suggests good surface passivation by the oleate ligands. We did not observe any secondary (trap-related) emission peak in PL, and the PL intensity remained stable (with no significant drop) over at least several weeks when the samples were stored under inert conditions in the dark. This implies that as-synthesized QDs have relatively few surface trap states initially, and that the oleic acid capping provides a degree of protection against immediate oxidation or photodegradation. However, we did not carry out comprehensive long-term stability tests or deliberate oxidation/photobleaching experiments. It is likely that exposure to air, moisture, or prolonged UV excitation would eventually lead to oxidation of the QD surface (e.g., forming CdO or TeO_2) and a corresponding decline in optical quality, as is known for many II–VI QDs without additional protective shells. In future work, systematic stability studies (such as monitoring PL intensity and peak position over time under various storage conditions, and performing photobleaching assays under continuous illumination) should be conducted to quantify the long-term colloidal and photostability of these CdTe QDs. Additionally, further improvements in stability and quantum yield could be achieved by overcoating the CdTe cores with a wider-bandgap shell. For example, growing a CdTe/ZnS core–shell structure (as conceptually depicted in Figure 1 after the core formation step) can dramatically enhance the QD's resistance to oxidation and increase QY by confining excitons away from surface defects. Although shell growth was outside the scope of this study, core/shell CdTe QDs are well known to exhibit superior stability and brightness [13].

Theoretical interpretation. The size-dependent spectral shifts we observe are consistent with the effective mass approximation (EMA) for semiconductor nanocrystals. The Brus equation provides a quantitative estimate of the first-exciton energy as a function of radius, capturing quantum-confinement effects. Using literature parameters for CdTe (electron effective mass $\approx 0.096\ m_0$, hole effective mass $\approx 0.60\ m_0$, and the bulk dielectric constant) [18], a 3 nm QD is expected to have a first-exciton energy near 2.4 eV (≈ 515 nm), while a 5 nm QD is expected near 1.9 eV (≈ 653 nm). These estimates agree with the absorption peaks of our smallest and largest samples. More sophisticated models could include surface strain, ligand-field effects, and dielectric screening (which can induce slight red shifts), but the EMA captures the dominant trends in our data.

Overall, our findings confirm that the molecular precursor (hot-injection) method is a powerful technique for producing high-quality CdTe QDs with controllable size. The combination of a rapid injection and proper ligand capping yields nanocrystals whose optical properties can be finely tuned, which is crucial for optimizing QDs for specific applications. In the next section, we summarize the conclusions and also outline some remaining challenges and future directions.

CONCLUSIONS

In summary, we have successfully synthesized CdTe quantum dots using a molecular precursor (TOP-Te) hot-injection method and investigated their optical properties as a function of particle size. By adjusting the growth time from 3 min to 16 min at 180 °C, we obtained a series of QD samples with tunable emission across the visible spectrum (from green to red). UV–Vis and PL spectroscopy confirmed a pronounced red-shift in absorption and emission peaks with increasing QD size, in agreement with quantum confinement theory. The CdTe QDs exhibit narrow excitonic absorption peaks and bright, size-dependent photoluminescence with high quantum yields (up to ~90%), indicating good crystalline quality and effective surface passivation by oleate ligands. These experimental observations were consistent with theoretical expectations (as estimated by the Brus equation) and with literature reports, validating the effectiveness of the relatively mild hot-injection synthesis approach for CdTe.

Direct structural and morphological characterization supported these findings: XRD confirmed the cubic CdTe phase and nanocrystal domain size, and TEM provided direct visualization of particle sizes (~3–5 nm) and their distribution, consistent with optical estimates. A logical next step is time-resolved PL to probe recombination dynamics and to test explicitly for trap-state contributions via exciton lifetimes. We also plan extended stability studies—exposure to air, light, and elevated temperature over longer periods—to assess long-term colloidal stability and resistance to photobleaching. The results will guide strategies such as core–shell encapsulation and optimized ligand treatments to enhance robustness. Finally, translating these QDs into aqueous media is important for specific uses; although we did not pursue ligand exchange here, future work should explore replacing oleate with hydrophilic ligands (or other phase-transfer methods) to yield water-dispersible CdTe QDs. Such surface modifications, together with protective shells, will broaden the applicability of these materials in optoelectronics, biology, and beyond.

ORCID

Karimberdi E. Onarkulov, https://orcid.org/0000-0002-8916-978X; **Adkhamjon I. Zokirov**, https://orcid.org/0000-0003-1651-1115

REFERENCES

[1] K.D. Wegner, and U. Resch-Genger, "The 2023 Nobel Prize in Chemistry: Quantum dots. Analytical and Bioanalytical Chemistry," **416**(14), 3283–3293 (2024). https://doi.org/10.1007/s00216-024-05225-9
[2] W. Li, "Quantum Dots for Biological Imaging," in: *Molecular Imaging. Advanced Topics in Science and Technology in China*, (Springer, Berlin, Heidelberg, 2023), pp. 501–511. https://doi.org/10.1007/978-3-642-34303-2_14
[3] Z. Ren, and J. Zhang, "Applications of fluorescent biosensors based on quantum dots," Highlights in Science, Engineering and Technology, **3**(1), 93-100 (2022). https://doi.org/10.54097/hset.v3i.697
[4] N. Ilaiyaraja, S.J. Fathima, and F. Khanum, "Quantum dots: A novel fluorescent probe for bioimaging and drug delivery applications," in: *Inorganic Frameworks as Smart Nanomedicines*, (William Andrew Publishing, 2018), pp. 529–563. https://doi.org/10.1016/B978-0-12-813661-4.00012-2
[5] E. Fresta, V. Fernández-Luna, P.B. Coto, and R.D. Costa, "Merging biology and solid-state lighting: Recent advances in light-emitting diodes based on biological materials," Advanced Functional Materials, **28**(24), 1707011 (2018). https://doi.org/10.1002/adfm.201707011
[6] J. Chen, H. Ding, and X. Sheng, "Advanced manufacturing of microscale light-emitting diodes and their use in displays and biomedicine," Journal of Information Display, **25**(1), 1–12 (2023). https://doi.org/10.1080/15980316.2023.2248403
[7] M. Green, "The origin and evolution of molecular precursors for quantum dot synthesis," Materials Advances, **5**(18), 7130–7139 (2024). https://doi.org/10.1039/d4ma00352g
[8] Y. Kwon, J. Oh, E.J. Lee, S.H. Lee, A. Agnes, G. Bang, J. Kim, *et al*., "Evolution from unimolecular to colloidal-quantum-dot-like character in chlorine- or zinc-incorporated InP magic-size clusters," Nature Communications, **11**(1), 3127 (2020). https://doi.org/10.1038/s41467-020-16855-9
[9] E. Lee, Y. Kwon, A. Agnes, Y. Ryu, and S. Kim, "Multiple roles of magic-sized clusters in quantum dot synthesis," Journal of Physical Chemistry C, Phys. Chem. C, **128**(4), 1809–1818 (2024). https://doi.org/10.1021/acs.jpcc.3c07189
[10] Y. Wang, B. Si, S. Lu, X. Ma, E. Liu, J. Fan, X. Li, and X. Hu, "Effective improvement in optical properties of colloidal CdTe@ZnS quantum dots synthesized from aqueous solution," Nanotechnology, **27**(36), 365707 (2016). https://doi.org/10.1088/0957-4484/27/36/365707
[11] H.H. Kim, J.-S. Park, I.K. Han, S.O. Won, C. Park, D.K. Hwang, and W.K. Choi, "Emissive CdTe/ZnO/GO quasi-core–shell–shell hybrid quantum dots for white light-emitting diodes," Nanoscale, **8**(47), 19737–19743 (2016). https://doi.org/10.1039/C6NR06314D
[12] X. Zhang, Y. Li, Y. Pan, and Q. Zhao, "Synthesis of water-soluble CdTe quantum dots and its influencing factors," Journal of Functional Materials, **43**(5), 667–670 (2012). https://doi.org/10.3969/j.issn.1004-1656.2012.05.002
[13] X.L. Liao, N. Yang, L.X. Xie, X.C. Yang, and X.P. Yang, "Synthesis and characterization of CdTe quantum dots capped by N-acetyl-L-cysteine," Applied Mechanics and Materials, **275–277**, 1956–1959 (2013). https://doi.org/10.4028/www.scientific.net/AMM.275-277.1956
[14] B. Zhou, F. Yang, X. Zhang, W. Cheng, W. Luo, L. Wang, and W. Jiang, "One-pot aqueous phase synthesis of CdTe and CdTe/ZnS core/shell quantum dots," Journal of Nanoscience and Nanotechnology, **16**(6), 5755–5760 (2016). https://doi.org/10.1166/jnn.2016.11764
[15] C.B. Murray, D.J. Norris, and M.G. Bawendi, "Synthesis and characterization of nearly monodisperse CdE (E = S, Se, Te) semiconductor nanocrystallites," Journal of the American Chemical Society, **115**(19), 8706–8715 (1993). https://doi.org/10.1021/ja00072a025
[16] P.F.G.M. da Costa, L.G. Merízio, N. Wolff, H. Terraschke, and A.S.S. de Camargo, "Real-time monitoring of CdTe quantum dots growth in aqueous solution," Scientific Reports, **14**(1), 1160 (2024). https://doi.org/10.1038/s41598-024-57810-8
[17] Y. Shi, Z. Ma, N. Cui, Y. Liu, X. Hou, W. Du, and L. Liu, "In situ preparation of fluorescent CdTe quantum dots with small thiols and hyperbranched polymers as co-stabilizers," Nanoscale Research Letters, **9**(1), 121 (2014). https://doi.org/10.1186/1556-276X-9-121
[18] M.P. Campos, and J.S. Owen, "Synthesis and surface chemistry of cadmium carboxylate-passivated CdTe nanocrystals from cadmium bis(phenyltellurolate)," Chemistry of Materials, **28**(1), 227–233 (2016). https://doi.org/10.1021/acs.chemmater.5b03914
[19] L. Ding, Z. Peng, W. Sun, T. Liu, Z. Chen, M. Gauthier, and F. Liang, "Microwave synthesis of CdTe/TGA quantum dots and their thermodynamic interaction with bovine serum albumin," Journal of Wuhan University of Technology–Materials Science Edition, **31**(6), 1408–1414 (2016). https://doi.org/10.1007/s11595-016-1546-x

СИНТЕЗ КВАНТОВИХ ТОЧОК CdTe МЕТОДОЮ МОЛЕКУЛЯРНИХ ПОПЕРЕДНИКІВ ТА ДОСЛІДЖЕННЯ ЇХ ОПТИЧНИХ ВЛАСТИВОСТЕЙ

Карімберді Е. Онаркулов, Адхамджон І. Зокіров
Ферганський державний університет, Фергана, Узбекистан

Квантові точки (КТ) телуриду кадмію (CdTe) були синтезовані методом молекулярного прекурсора (гарячої інжекції) та досліджені їхні оптичні властивості. Прекурсор олеату кадмію в октадецені/олеїновій кислоті нагрівали до 180°C в інертній атмосфері, а розчин триоктилфосфіну-телурію (TOP-Te) швидко вводили для ініціювання нуклеації. Змінюючи час росту (3-16 хв), розмір КТ налаштовували, створюючи кольори випромінювання від зеленого до червоного. Нанокристали були охарактеризовані за допомогою УФ-Vis абсорбційної та фотолюмінесцентної (ФЛ) спектроскопії, яка показала чітке червоне зміщення оптичних спектрів зі збільшенням розміру частинок. Квантові точки CdTe демонструють оптичні властивості, що залежать від розміру, що узгоджуються з квантовим обмеженням, причому перший екситонний пік поглинання зміщується від ~520 нм до ~700 нм зі збільшенням діаметра. Всі зразки були високолюмінесцентними, зі значеннями квантового виходу фотолюмінесценції (PLQY) в діапазоні 60–90%. Цей простий синтез при відносно низькій температурі дає колоїдно стабільні квантові точки CdTe з настроюваними забороненими зонами. Результати демонструють простий шлях до налаштування оптичних властивостей квантових точок шляхом контролю часу реакції та дають уявлення про кінетику росту та квантово-розмірні ефекти в квантових точках CdTe.

Ключові слова: *квантова точка; телурид кадмію; молекулярний прекурсор; гаряча інжекція; квантове обмеження; фотолюмінесценція; поглинання; нанокристал; колоїдний синтез; напівпровідник*